Variability of D and H in the Martian upper atmosphere observed with the MAVEN IUVS echelle channel

John T. Clarke, Mayd Mayyasi, Dolon Bhattacharyya, Nicholas M. Schneider, William E. Mcclintock, Justin I. Deighan, A. Ian F. Stewart, Jean-Yves Chaufray, Michael S. Chaffin, Sonal Kumar Jain, et al.

AGU PUBLICATIONS

JGR

Journal of Geophysical Research: Space Physics

RESEARCH ARTICLE
10.1002/2016JA023479

Special Section:
Major Results From the MAVEN Mission to Mars

Variability of D and H in the Martian upper atmosphere observed with the MAVEN IUVS echelle channel

J. T. Clarke[1], M. Mayyasi[1], D. Bhattacharyya[1], N. M. Schneider[2], W. E. McClintock[2], J. I. Deighan[2], A. I. F. Stewart[2], J.-Y. Chaufray[3], M. S. Chaffin[2], S. K. Jain[2], A. Stiepen[4], M. Crismani[2], G. M. Holsclaw[2], F. Montmessin[3], and B. M. Jakosky[2]

[1]Center for Space Physics, Boston University, USA, [2]LASP, Univ. of Colorado, USA, [3]LATMOS, France, [4]LPAP, Univ. of Liège, Belgium

Key Points:
- First observations with the MAVEN IUVS echelle channel are presented
- H and D Ly α emissions from Mars are highly variable, both absolutely and with respect to each other
- Observations are consistent with large seasonal changes with implications for history of water escape

Supporting Information:
- Supporting Information S1

Correspondence to:
J. T. Clarke,
jclarke@bu.edu

Citation:
Clarke, J. T., et al. (2017), Variability of D and H in the Martian upper atmosphere observed with the MAVEN IUVS echelle channel, *J. Geophys. Res. Space Physics*, *122*, 2336–2344, doi:10.1002/2016JA023479.

Received 16 SEP 2016
Accepted 24 JAN 2017
Accepted article online 28 JAN 2017
Published online 15 FEB 2017

Abstract The MAVEN IUVS instrument contains an echelle spectrograph channel designed to measure D and H Ly α emissions from the upper atmosphere of Mars. This channel has successfully recorded both emissions, which are produced by resonant scattering of solar emission, over the course of most of a martian year. The fundamental purpose of these measurements is to understand the physical principles underlying the escape of H and D from the upper atmosphere into space, and thereby to relate present-day measurements of an enhanced HDO/H_2O ratio in the bulk atmosphere to the water escape history of Mars. Variations in these emissions independent of the solar flux reflect changes in the density and/or temperature of the species in the upper atmosphere. The MAVEN measurements show that the densities of both H and D vary by an order of magnitude over a martian year, and not always in synch with each other. This discovery has relevance to the processes by which H and D escape into space. One needs to understand the controlling factors to be able to extrapolate back in time to determine the water escape history from Mars at times when the atmosphere was thicker, when the solar flux and solar wind were stronger, etc. Further measurements will be able to identify the specific controlling factors for the large changes in H and D, which likely result in large changes in the escape fluxes of both species.

1. Introduction

The global deuterium to hydrogen (D/H) ratio of the martian atmosphere, as determined by spectroscopic measurements of HDO and H_2O in the lower atmosphere, is roughly 5 times higher than in the terrestrial atmosphere [*Owen et al.,* 1988], with a range of values measured at different seasons and latitudes [*Aoki et al.,* 2015; *Encrenaz et al.,* 2016; *Krasnopolsky*, 2015; *Villanueva et al.,* 2015]. This has been widely interpreted as resulting from the escape of a large volume of water into space, with the majority loss early in the history of Mars [*Yung et al.,* 1988; *Yung and Kass,* 1998]. Since H atoms escape the planet's gravity faster than D atoms due to the mass difference, the overall D/H ratio will increase with time as more water is lost. The present D/H ratio can be related to the total amount of water lost into space, and thus the amount of water present on ancient Mars, with one key assumption. The measured D/H ratio reflects the reservoir of water that condenses and sublimates seasonally from the surface, and this is the main reservoir of water on Mars. Additional water in the crust that has not participated in the cycling process since ancient times could have a different D/H ratio, and reflect a different water history on early Mars. In this sense the interpretation of the D/H ratio today applies to the surface water that exchanges with the atmosphere over the course of the seasons, and reflects a lower limit to the quantity of ancient water.

Mars is known to have experienced large climate changes over time. To be able to accurately extrapolate the water history back in time it is important to determine by measurement the physical processes that control the escape rates of H and D today, so that one can model the rates of escape under past conditions of solar flux, atmospheric conditions, etc. [*Lillis et al.,* 2015]. This work is one of the main scientific objectives of the Mars Atmosphere Volatile EvolutioN (MAVEN) mission to Mars [*Jakosky et al.,* 2015].

The MAVEN Imaging Ultraviolet Spectrograph (IUVS) instrument includes a far-UV spectral channel that employs an echelle grating to separately measure the brightness of resonantly scattered solar Ly α emissions by H and D atoms in the martian upper atmosphere. These values can be related to the density and temperature of H and D above the altitude where photoabsorption by CO_2 becomes optically thick to this radiation (~80-100 km at nadir and ~100-120 km in limb-viewing). This far-UV measurement thus samples both the

bound and escaping atoms, and is complementary to ground-based IR observations of HDO and H_2O in the lower atmosphere. The density, temperature, and altitude profiles of H and D are derived from the brightness measurements through the use of a radiative transfer model for multiple scattering of the solar photons [*Chaufray et al.,* 2008; *Bhattacharyya et al.,* 2016].

Early observations of the H Ly α emission from Mars were interpreted as reflecting a steady rate of H loss into space [*Anderson,* 1974]. Early models assumed that H_2O and HDO were photodissociated by UV sunlight near the surface and collisionally recombined into H_2 and HD, which then slowly diffused upward [*Yung et al.,* 1988]. At high altitudes these species would be dissociated by ion chemical reactions into atomic form [*Krasnopolsky et al.*, 1998]. A non-negligible portion of the high-energy tail of these H atoms' velocity distribution can exceed Mars' escape velocity and hence escape to space on a relatively shorter time scale (i.e. Jeans escape) [*Chamberlain,* 1963; *Hunten,* 1973]. In this picture, water was believed to be efficiently trapped close to the surface by condensation in the atmosphere [*Bertaux and Montmessin,* 2001], and the bottleneck for escape of hydrogen was the slow upward diffusion of H_2 with a time scale of months [*Clarke et al.,* 2014]. While the initial observations were of water, it is D, H, and O that escape the atmosphere, and these atomic species are best observed at far-UV wavelengths.

Prior observations of both the H and D Ly α emissions have been performed on 3 occasions using two different instruments with echelle channels on the Hubble Space Telescope (HST). Initial observations with the Goddard High Resolution Spectrograph (GHRS) instrument on 22 May 1991 ($L_S = 63$) found a 30 Rayleigh (R) D emission Doppler-shifted from the terrestrial D line, which appeared at a comparable brightness [*Bertaux et al.*, 1993]. In these observations of the sunlit disc of Mars the H brightness was 8 kilo-Rayleighs (kR). Later GHRS observations pointed at the sunlit limb of Mars on 20 Jan. 1997 ($L_S = 67$) found a D brightness of 47 R, including an assumed limb brightening factor, and an H brightness of 3.3 kR [*Krasnopolsky et al.,* 1998]. Both of these works found D/H ratios comparable (within the uncertainties) with the factor of 5 enhancement measured in lower atmospheric HDO / H_2O. Later observations were obtained with the Space Telescope Imaging Spectrograph (STIS) instrument, with a long aperture obtaining spatially-resolved spectra across the disc of Mars. In these data the D brightness was 35 R and the H brightness was 9 kR in averages across the sunlit disc, and a radiative transfer model found a D/H enhancement over terrestrial water that was comparable to or somewhat larger than the other measurements within the uncertainty [*Clarke et al.,* 2006]. All of these observations suggested that the upper atmospheric ratio of atomic D/H was comparable within a factor of two of the value measured in lower atmospheric deuterated water.

More recently, but prior to the arrival of MAVEN at Mars, HST and Mars Express (MEX) measurements of the martian H corona showed large (order of magnitude) changes in the H exosphere and escape flux over the course of a martian orbit about the Sun [*Clarke et al.,* 2014; *Chaffin et al.,* 2014; *Bhattacharyya et al.,* 2015]. The maximum H density was seen in late southern summer when the overall atmosphere was most convectively active. A seasonal increase of the H escape flux driven mainly by the increase of the solar EUV flux was simulated by *Chaufray et al.* [2015]. They found an expected variation lower than the observed magnitude, suggesting that an additional process is needed to explain the observations. The observed increase is consistent with a direct injection of hydrogen atoms from dissociation of high altitude water, although the detailed controlling factors have not been determined. Measurements from the SPICAM instrument on Mars Express showed that water was at times super-saturated in the middle atmosphere, and reached altitudes above 60 km at substantial densities [*Fedorova et al.,* 2009; *Maltagliati et al.,* 2013]. This strong seasonal change had not been predicted, and to understand the process of atmospheric escape, the hydrogen abundance in the upper atmosphere needs to be measured over a full martian year. To relate the evolution of the D/H ratio to the water escape flux, both H and D need to be measured. Since a large increase in the Ly α brightness has been detected post-perihelion in two prior martian years, a similar seasonal pattern was expected to be observed by MAVEN. There are now sufficient IUVS echelle data to establish the trend in H and D emissions over most of a seasonal cycle, and these results are reported in this paper.

2. Instrument and Observations

The IUVS instrument on MAVEN contains an echelle spectrograph with a novel optical design to enable long-aperture measurements of emission lines, intended primarily to measure the H and D Ly α emission lines from the martian upper atmosphere [*McClintock et al.,* 2015]. The main scientific goal of the echelle channel is to

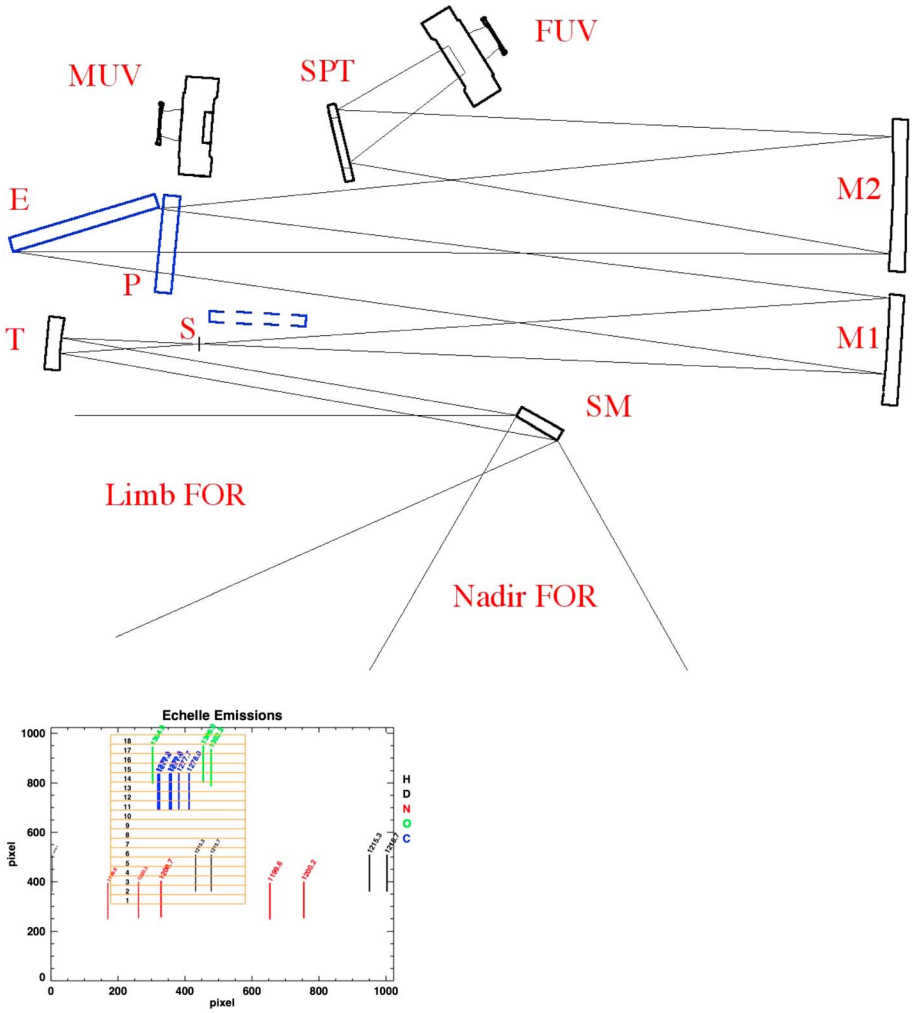

Figure 1. Schematic of the optical/mechanical layout of the IUVS instrument showing the light path through the echelle mode (upper), and the layout of the main spectral lines on the detector (lower). In the upper panel, FOR is the field of regard, SM is a scan mirror, T the telescope mirror, S the entrance slit, M1 and M2 are collimating and focusing mirrors, P the prism, E the echelle grating, SPT a beam splitter, and FUV the far-UV detector. In the lower panel the echelle dispersion is horizontal and the prism cross dispersion is vertical. The region marked by yellow lines shows the binned area of data that was downloaded in the initial phase of the MAVEN mission. The D and H emission lines are the central vertical black lines in the lower panel.

measure these emissions, which result from resonant scattering of solar emission, and to discover how the H and D densities, temperatures, and escape fluxes vary with factors such as local time, solar zenith angle and solar activity, season, and topography.

To accomplish this goal a spectral channel with an echelle grating was added to the instrument, whose design has been based on a sounding rocket experiment that first employed a long aperture to image an emission line spectrum without continuum, and using an objective prism for the cross dispersion [*Harris et al.,* 1993]. The implementation into the IUVS instrument package is described by *McClintock et al.* [2015]. The principle of operation takes advantage of the fact that the far-UV spectrum of Mars contains widely spaced emission lines with no continuum emission. In the absence of continuum, adjacent spectral orders of the echelle grating appear in the spectral format only at the wavelengths of the emission lines, and a long narrow aperture can be employed for high count rates from diffuse emissions. The cross dispersion in the echelle spectral format was accomplished with an objective prism rather than a grating. This greatly simplified the optical design and allowed its inclusion in the IUVS instrument package. The length of the entrance aperture in the echelle format is limited to 0.9° to avoid overlap of different lines, and the emission spectrum

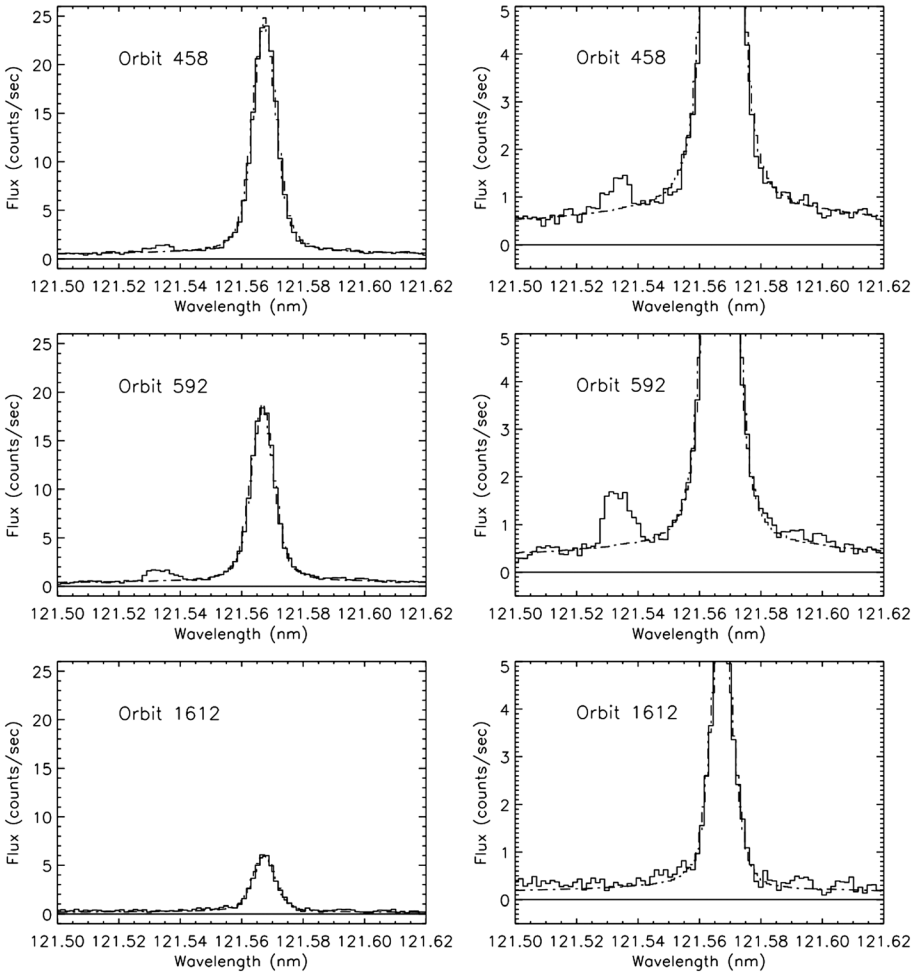

Figure 2. IUVS echelle spectra of the sunlit disc of Mars during orbits 458 (24 Dec. 2014), 592 (19 Jan. 2015), and 1612 (28 July 2015) showing the spectrally separated H (121.567 nm) and D (121.533 nm) Ly α emissions on two intensity scales. Each spectrum is from roughly 300 sec. of integration time, and the dashed lines are fits of the instrument line spread function (LSF) to the H line. Once this has been subtracted, the D emission flux is derived by re-setting the local background level and fitting the LSF to the D emission. The uncertainty in the measurement is obtained by performing the same LSF fit to wavelength intervals devoid of emission, and finding the mean and standard deviation in the derived fluxes. The large variations in both emissions can clearly be seen in these plots.

appears on the detector as widely separated features with the aperture filled with diffuse emissions at different wavelengths [Figure 1].

The spectral resolution is limited by the aperture width, with a dispersion of 0.000737 nm/pixel and a spectral resolution of 0.008 nm (20 km/sec) full width at half maximum. This resolution is too coarse to resolve the intrinsic width of the martian emission line, but sufficient to separate the main emissions and their multiplets from the martian airglow and to resolve doppler-broadened emissions from sources such as the interplanetary hydrogen [*Quemerais and Bertaux*, 1993] and comets [*Combi et al.,* 1996]. The H and D Ly α lines at 121.5671 and 121.3331 nm are separated by 8 resolution elements, and the faint D emission line appears on the blue wing of the grating scattered light from the brighter H line [Figure 2]. The echelle spectra have been reduced starting with the level_1a data products, and details of the reduction procedures and the measured properties of the echelle channel are given in *Mayyasi et al.* [2016].

The echelle spectra are recorded on a two-dimensional microchannel plate detector that employs an active pixel sensor readout device [*McClintock et al.,* 2015]. We have experimented extensively with different methods to filter out both cosmic ray and thermal noise on the detectors toward the goal of having the best sensitivity to the faint D emissions. The count rates in the echelle mode are a factor of 8 lower than in the low

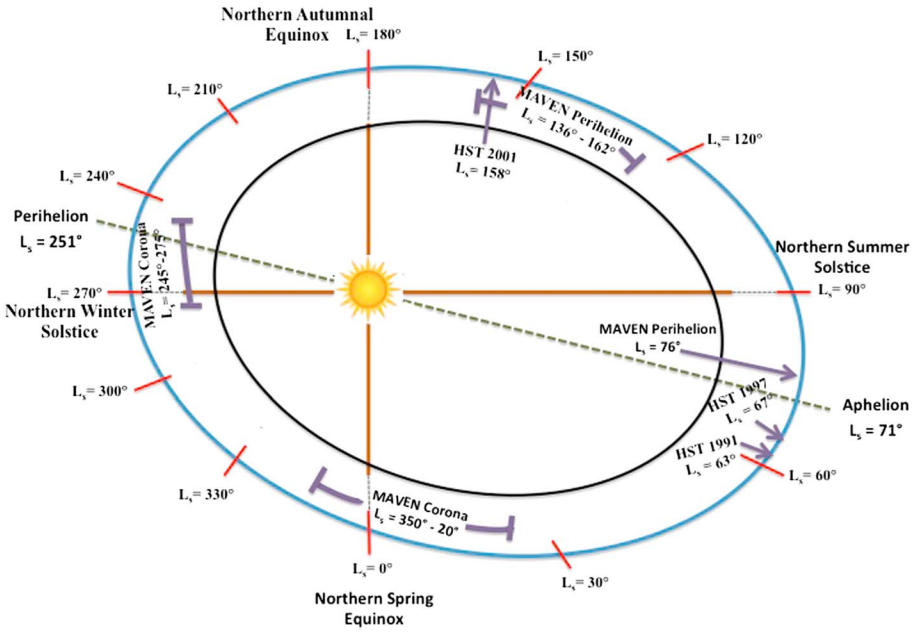

Figure 3. Range of martian seasons and solar longitude L_S during IUVS echelle observations. HST observations of the H and D Ly α emissions are generally consistent with the seasonal changes detected by the IUVS, although with only 3 observation times of the D emission.

resolution FUV mode of the IUVS [*Mayyasi et al.,* 2016], requiring correspondingly longer integration times for equivalent signal to noise measurement. The absolute sensitivity calibration of the echelle mode presented here is provisional, and is based on comparison of the interplanetary hydrogen emission brightness with observations by the SWAN experiment on SOHO [*Quemerais and Bertaux*, 1993], observations of the sunlit martian disc compared with HST [*Bhattacharyya et al.,* 2015], and consistency with the IUVS FUV mode in observations of flux calibration stars [see discussion in *Mayyasi et al.,* 2016]. Future modest changes in the brightness calibration will not affect the conclusions of this paper, which are based on the emission brightness changes over time. A high stability of the response of the echelle channel has been determined by comparing the count rates of the echelle and FUV modes, along with repeated FUV observations of calibration stars.

Observations with the echelle mode have been performed with a variety of observing geometries and detector pixel binning schemes, which have been required to limit the data rate in the communication bandwidth from the spacecraft to the Earth. The initial data reported here are from observations scanning across the sunlit martian disc and limb on the outgoing portion of the MAVEN orbit (called "coronal scans", MAVEN orbits 337–1644). As Mars moved farther from the Sun, both the H and D emissions became much fainter, and the D emission fell below the detection limit in this mode. In addition, after orbit 1644 the sunlit disc could no longer be observed in the coronal scan portion of the MAVEN orbit due to the changing orbital geometry. Starting with orbit 2288, the observations were changed to view only the sunlit limb during the periapse portion of the orbit (called "periapse scans", orbits 2288–3261), giving a higher sensitivity due to the limb brightening enhancement of the faint optically thin D emission. The details of the observations including specific pointing are given in the supplementary table. The brightnesses in the two observing modes are not directly comparable, but similar enough to determine the large overall variation in emission brightness observed over the martian year.

3. Variations in Measured D and H Emissions

Examples of individual spectra of the H and D Ly α emissions from the coronal scan observations are shown in Figure 2. The D line appears shifted 0.034 nm from the H line on the wing of the grating scattered light profile, and the D emission is much fainter than the H emission. Early in the MAVEN mission the D line was unexpectedly bright and easily measured. The D emission brightness increased over orbits 337–596 while the H

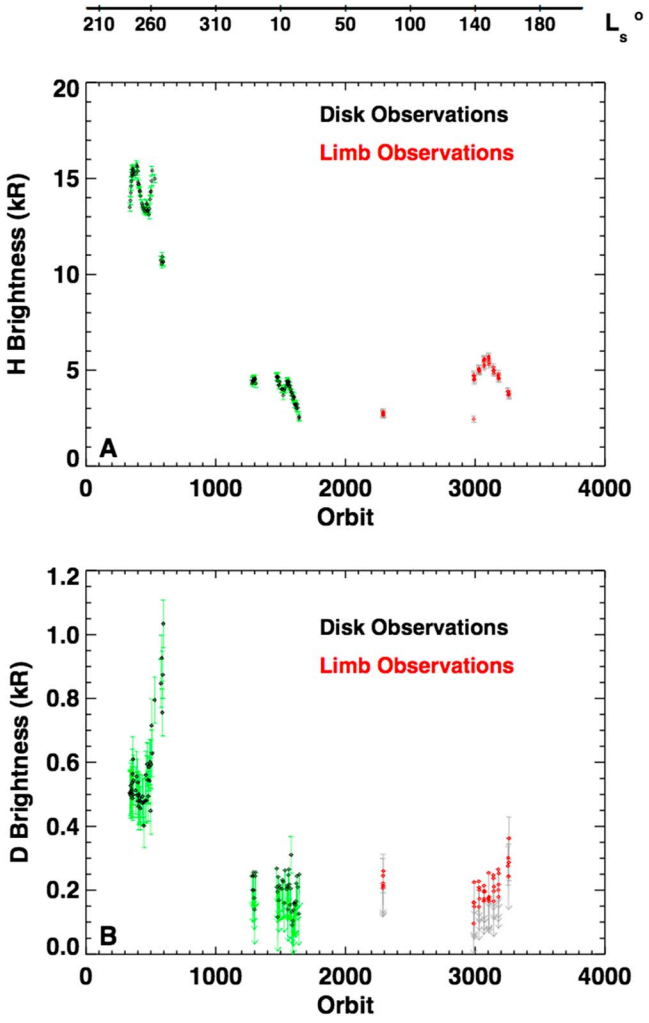

Figure 4. Measured brightnesses of the H and D emissions versus MAVEN orbit number observed with the IUVS echelle channel during coronal scans of the sunlit disc of Mars (disk) (orbits 337–1644) and during periapse limb scans "Limb" (orbits 2288–3261) with one sigma error bars. The coronal and periapse scans are not directly comparable due to different observing geometries. On time scales of weeks to months both emissions decrease with increasing distance of Mars from the Sun, and the solar rotation period is seen in short-term changes in brightness.

emission became fainter, potentially due to an increase in D and or H near the terminator [*Chaffin et al.,* 2015]. By orbit 1280 the D emission was too faint to be detected. On switching to periapse limb scans starting with orbit 2288 the D emission was once more detected owing to the limb enhancement. While the observations need to be carefully modeled to derive quantitative densities, the overall trend in brightness is clear. The range of martian orbital positions where observations have been obtained is shown in Figure 3.

The entire data set is plotted in Figure 4, showing the trend over solar longitudes 240 through zero to 160 (near perihelion in late southern summer through aphelion to early southern summer). Over orbits 337–596 a variation with the solar rotation was seen in the H emission, which varied with a 28 day period, and to a less clear extent in the fainter D emission. This variation is consistent with MAVEN EUVM measurements of the solar Ly α flux at Mars, and this reflects changes in the solar emission and not the martian upper atmosphere [*Eparvier et al.,* 2015]. There is also an increase in D emission over orbits 400–600 that is not matched by an increase in the H emission. At this time the line of sight was moving toward larger solar zenith angles. An increase in the He density near dawn and dusk has been found in the MAVEN NGIMS data [*Elrod et al.,* 2017]. This helium "bulge" is consistent with global circulation models [*Bougher et al.,* 2015], and there may be a corresponding D bulge near the terminator that appears in the echelle data. Further observations will test whether this is a persistent feature near the terminators.

We can conclude from the trends in Figure 4 that the H and D emissions exhibit a strong temporal variation (likely seasonal variability in H and D), that they do not always vary together (e.g. over orbits 500–600), and that the ratio of D to H brightness is not constant. The measured brightness depends on the solar Ly α flux at Mars and also on the observing geometry, and these factors have been modeled using a radiative transfer code [*Bhattacharyya et al.,* 2016]. Figure 5 shows the ratio of the observed brightness to the modeled values assuming that the martian atmosphere is spherically symmetric and did not change in density or temperature. The solar Ly α flux at line center for the modeled MAVEN orbits were obtained by applying the relation presented in *Emerich et al.* [2005] to the line-integrated Lyman α flux from the SORCE database [*Rottman et al.,* 2006], corrected for solar rotation and distance to Mars. The atmospheric temperature is taken from modeling for the value at the subsolar point for this season and solar activity [*Bougher et al.,* 2015], and the density is

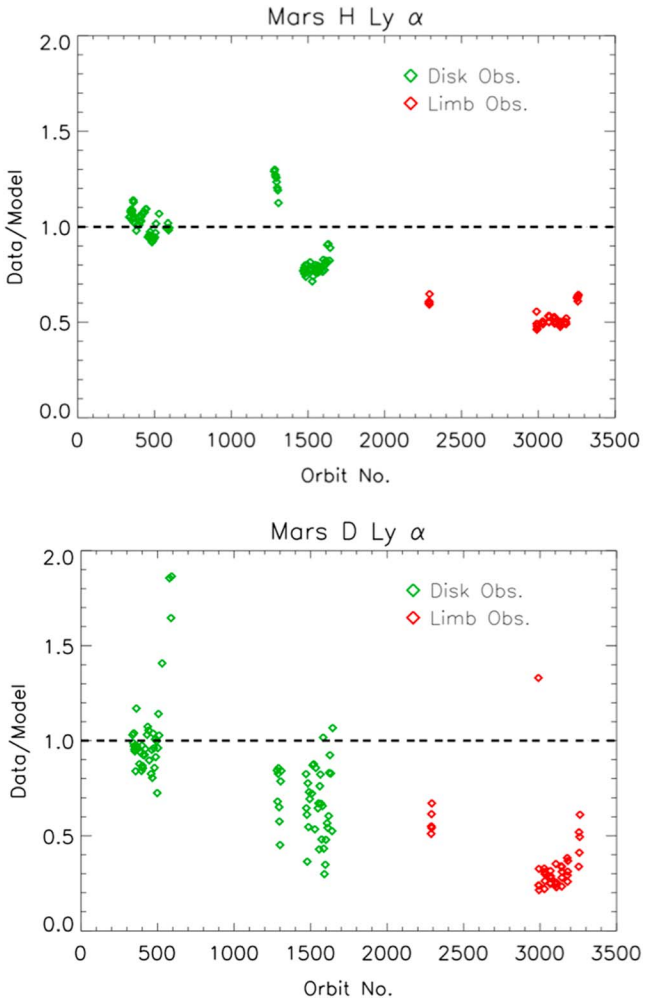

Figure 5. Mars H and D Ly α emission brightness changes as ratios to the values expected from the results of a radiative transfer model. The model assumes spherical symmetry in the martian upper atmosphere and no changes in density and temperature, and it takes into account the changing solar Ly α flux at Mars. The ratios of both emissions show decreasing trends with time, and continue to decrease after Mars aphelion (on Nov. 20, 2015 or around orbit 2230). The brightness changes are more pronounced than expected from the changing solar Ly α flux at Mars and the changing observing geometry.

then adjusted to fit the brightness in the first data points. More details of the modeling are given in the supplementary material. There is considerable scatter in the data from orbit to orbit, likely due to some combination of local time variations in the H and D abundances [*Chaufray et al.,* 2015] and noise in the data (note that the level of scatter is larger for the fainter D emission). Prior IUVS observations have shown that the H distribution exhibits significant local time variations in density and temperature [*Chaffin et al.,* 2015], which have not been considered in this initial modeling. In addition to these short-term changes, however, there also appears a clear long-term trend of decreasing brightness in Figure 5 and thereby in the properties of both H and D in the martian upper atmosphere.

3.1. Interpretation and Discussion

The H line is optically thick, while the D line is optically thin, and the brightness of the Ly α emissions depends on the atomic density and temperature and the line of sight through the atmosphere [see detailed discussion in *Bhattacharyya et al.,* 2016]. A careful radiative transfer analysis is required to determine the atomic D/H density ratio in the upper atmosphere and how it has changed with time. For now, however, it is clear that the unexpectedly bright D emission observed early in the MAVEN mission is well above that seen in earlier HST observations, and the much higher ratio of D to H brightnesses implies a D/H enhancement that is correspondingly larger than the factor of 5 seen in low altitude water. As the D emission decreased in brightness over time, it dropped closer to the level seen in the three HST observations described below, and the H emission brightness was also similar to the HST data. The D/H ratio in the later data can be expected to be similar to that of low altitude martian water, consistent with the HST data analyses. The D emission decreased by more than a factor of 5 in these observations (uncertainty due to upper limits), and if the change were entirely due to a decrease in D density the change would be comparable. For the optically thick H emission, the observed decrease of a factor of 4 would correspond under the same assumption to a much larger fractional decrease in density [*Bhattacharyya et al.,* 2016]. A more detailed radiative transfer analysis will be needed to refine these numbers.

Three prior HST observations obtained with the GHRS and STIS instruments in their echelle modes measured the H and D Ly α emissions [*Bertaux et al.,* 1993; *Krasnopolsky et al.,* 1998; *Clarke et al.,* 2006]. The H emission was roughly 3–6 kR, similar to the fainter MAVEN measurements presented here. The D emission was in the range 20–50 R, somewhat fainter than the MAVEN detection limit near aphelion. The HST observations were

also obtained either near martian aphelion or in late northern summer ($L_S = 63$, 67, and 158), and the HST observing conditions were with a small field of view on the sunlit disc from a large distance. The derived values of the D/H ratio based on modeling these data were consistent with the enhancement seen in the lower altitude HDO/H_2O within the uncertainties, however the HST echelle spectra were not obtained at the seasonal epoch when later HST images, MEX, and MAVEN IUVS data have shown Mars to be much brighter at Ly α (Figure 3). Given the timing of the various observations, the data appear consistent with a repeated large seasonal change in upper atmospheric hydrogen.

The H and D brightnesses presented in this paper are being modeled in more detail to more accurately determine the hydrogen densities and D/H ratio in the martian upper atmosphere, including changes in both density and temperature. It is already clear, however, that there is a large seasonal change in both the hydrogen densities and the D/H ratio in the upper atmosphere. Prior work has cited the likelihood of an infusion of water into the middle atmosphere (50–100 km) during southern summer seen in the MEX data [*Fedorova et al.,* 2015; *Maltagliati et al.,* 2013], in which case direct photodissociation by solar UV can provide a short-term source of H and D atoms into the upper atmosphere. In this event, with a more rapid escape rate for H than D due to the mass difference [*Montmessin et al.*, 2005], one might expect a temporary increase in the D/H ratio. The time scale for the loss of H and D atoms by Jeans escape from above 100 km is a few days, and the diffusion time for H_2 from the lower atmosphere is likely to be months, while the upwelling of water molecules into the middle atmosphere may occur on a time scale of days to weeks when the lower atmosphere is turbulent [*Clarke et al.,* 2014]. These times are short compared with the martian seasonal cycle, and over the long term the D/H ratio would be expected to return closer to the value in the overall atmosphere. This trend appears consistent with the later IUVS echelle data. More quantitative conclusions about the D/H ratio await the results of the more detailed radiative transfer calculations. It should also be kept in mind that fully understanding the details of D and H evolution in the Martian upper atmosphere over the annual cycle will require rigorous, detailed modeling beyond that currently employed.

4. Conclusions

This paper reports initial observations of D and H emissions in the martian upper atmosphere obtained with the MAVEN IUVS echelle channel. The basic operating principles of the echelle channel and the properties of the data are presented, with reference to a more detailed description of its calibration [*Mayyasi et al.,* 2016]. The brightnesses of the H and D Ly α emissions from Mars have shown unexpected variations, with the D emission initially much brighter than previously measured and both emissions decreasing by large factors as Mars moved away from perihelion. These data, along with prior measurements, are consistent with a repeated seasonal dependence of the hydrogen content in the martian upper atmosphere, potentially due to periodic increases in both species due to increased levels of water in the middle atmosphere arising from high levels of convective activity in late southern summer. This, has important implications for the factors that have controlled the long term escape of martian water into space. We expect to learn more from the H and D emissions and how they evolve over the course of the next perihelion passage over fall and winter 2016.

Acknowledgments

This work is based on observations with the NASA MAVEN spacecraft. These observations were supported by NASA grant NNH1OCCO4C under a subcontract to Boston University. J-Y Chaufray and F. Montmessin are supported by the Centre National d'Etudes Spatiales and A. Stiepen is supported by the Belgian Fund for Scientific Research (FNRS). The MAVEN data can be downloaded from the NASA Planetary Data System at http://atmos.nmsu.edu/data_and_services/atmospheres_data/MAVEN/echelle.html

References

Anderson, D. E. (1974), Mariner 6, 7, and 9 Ultraviolet Spectrometer Experiment: Analysis of Hydrogen Lyman Alpha Data, *J. Geophys. Res.*, *79*, 1513–1518, doi:10.1029/JA079i010p01513.

Aoki, S., H. Nakagawa, H. Sagawa, M. Giruanna, G. Sindoni, A. Aronica, and Y. Kasaba (2015), Seasonal Variation of the HDO/H_2O Ratio in the Atmosphere of Mars at the Middle of Northern Spring and Beginning of Northern Summer, *Icarus*, *260*, 7–22, doi:10.1016/j.icarus.2015.06.021.

Bertaux, J. L., and F. Montmessin (2001), Isotopic Fractionation through Water Vapor Condensation: the Deuterophase, a Cold Trap for Deuterium in the Atmosphere of Mars, *J. Geophys. Res.*, *106*(E12), 32,879–32,994, doi:10.1029/2000JE001358.

Bertaux, J. L., J. T. Clarke, M. J. Mumma, T. Owen, and E. Quemerais (1993), A Search for the Deuterium Lyman-alpha Emission from the Atmosphere of Mars, in *Science with the Hubble Space Telescope, ESO Proc. 44*, pp. 459–462.

Bhattacharyya, D., J. T. Clarke, J.-L. Bertaux, J.-Y. Chaufray, and M. Mayyasi (2015), A Strong Seasonal Dependence in the Martian Hydrogen Exosphere, *Geophys. Res. Lett.*, *42*, 8678–8685, doi:10.1002/2015GL065804.

Bhattacharyya, D., J. T. Clarke, J.-L. Bertaux, J.-Y. Chaufray, and M. Mayyasi (2016), Analysis and Modeling of Remote Observations of the Martian Hydrogen Exosphere, *Icarus*, *281*, 264–280, doi:10.1016/j.icarus.2016.08.034.

Bougher, S. W., D. Pawlowski, J. M. Bell, S. Nelli, T. McDunn, J. R. Murphy, M. Chizek, and A. Ridley (2015), Mars Global Ionosphere-Thermosphere Model: Solar Cycle, Seasonal, and Diurnal Variations of the Mars Upper Atmosphere, *J. Geophys. Res. Planets*, *120*, 311–342, doi:10.1002/2014JE004715.

Chaffin, M., et al. (2015), Three Dimensional Structure in the Martian H Corona Revealed by IUVS on MAVEN, *Geophys. Res. Lett.*, *42*, 9001–9008, doi:10.1002/2015/GL065287.

Chaffin, M. S., J. Y. Chaufray, I. Stewart, F. Montmessin, N. M. Schneider, and J. L. Bertaux (2014), Unexpected Variability of Martian Hydrogen Escape, *Geophys. Res. Lett.*, *41*, 314–320, doi:10.1002/2013GL058578.

Chamberlain, J. W. (1963), Planetary Coronae and Atmospheric Evaporation, *Planet. Space Sci.*, *11*, 901–960, doi:10.1016/0032-0633(63)90122-3.

Chaufray, J. Y., F. Gonzalez-Galindo, F. Forget, M. A. Lopez-Valverde, F. LeBlanc, R. Modolo, and S. Hess (2015), Variability of the Hydrogen in the Martian Upper Atmosphere as Simulated by a 3D Atmosphere-Exosphere Coupling, *Icarus*, *245*, 282–294, doi:10.1016/j.icarus.2014.08.038.

Chaufray, J.-Y., J.-L. Bertaux, F. Leblanc, and E. Quémerais (2008), Observation of the hydrogen corona with SPICAM on Mars Express, *Icarus*, *195*, 598–613, doi:10.1016/j.icarus.2008.01.009.

Clarke, J. T., J.-L. Bertaux, J.-Y. Chaufray, T. Owen, A. Nagy, and G. R. Gladstone (2006), HST/STIS Observations of the D/H Ratio in the Martian Upper Atmosphere, *Bull. Amer. Astr. Soc.*, *38*, 600.

Clarke, J. T., J. L. Bertaux, J. Y. Chaufray, G. R. Gladstone, E. Quemerais, J. K. Wilson, and D. Bhattacharyya (2014), A Rapid Decrease of the Hydrogen Corona of Mars, *Geophys. Res. Lett.*, *41*, 8013–8020, doi:10.1002/2014GL061803.

Combi, M. R., M. E. Brown, P. D. Feldman, H. U. Keller, R. R. Meier, and W. H. Smyth (1996), A Comprehensive Study of the H Lyman-alpha Line Profile and Water Photochemistry in Comet Hyakutake (1996 B2), *Bull. Amer. Astr. Soc.*, *28*, 1094.

Elrod, M. K., S. Bougher, J. Bell, P. R. Mahaffy, M. Benna, S. Stone, R. Yelle, and B. Jakosky (2017), He Bulge Revealed: He and CO_2 diurnal and seasonal variations in the Upper Atmosphere of Mars as detected by MAVEN NGIMS, *J. Geophys. Res. Space Physics*, *122*, doi:10.1002/2016JA023482.

Emerich, C., P. Lemaire, J.-C. Vial, W. Curdt, U. Schühle, and K. Wilhelm (2005), A new relation between the central spectral solar H I Lyman α irradience and the line irradience measured by SUMER/SOHO during the cycle 23, *Icarus*, *178*, 429–433, doi:10.1016/j.icarus.2005.05.002.

Encrenaz, T., et al. (2016), A Map of D/H on Mars in the Thermal Infrared using EXES aboard SOFIA, *Astr. Astrph.*, *586*, A62, doi:10.1051/0004-6361/201527018.

Eparvier, F., P. Chamberlin, T. N. Woods, and E. Thiemann (2015), The Solar Extreme Ultraviolet Monitor for MAVEN, *Space Sci. Rev.*, *195*, 293–301, doi:10.1007/s11214-015-0195-2.

Fedorova, A., O. Korablev, J.-L. Bertaux, A. V. Rodin, F. Montmessin, D. A. Belyaev, and A. Reberac (2009), Solar Infrared Occultation Observations by SPICAM Experiment on Mars-Express: Simultaneous Measurements of the Vertical Distributions of H_2O, CO_2, and Aerosol, *Icarus*, *200*, 96–117, doi:10.1016/j.icarus.2008.11.006.

Fedorova, A., J.-L. Bertaux, F. Montmessin, O. Korablev, I. Dzuban, L. Maltagliati, and J. Clarke (2015), Water Vapor in the Middle Atmosphere of Mars During the Global Dust Storm in 2007, *EGU General Assembly*, Vienna, Austria, 12–17 April.

Harris, W. M., J. T. Clarke, J. R. Caldwell, P. D. Feldman, B. C. Bush, D. M. Cotton, and S. Chakrabarti (1993), High Resolution Ultraviolet Spectrograph for Sounding Rocket Measurements of Planetary Emission Line Profiles, *Opt. Eng.*, *32*, 3016, doi:10.1117/12.149165.

Hunten, D. M. (1973), The Escape of Light Gases from Planetary Atmospheres, *J. Atmos. Sci.*, *30*, 1481–1494, doi:10.1175/1520-0469(1973)030<1481:TEOLGF>2.0.CO;2.

Jakosky, B. M., et al. (2015), The Mars Atmosphere and Volatile Evolution (MAVEN) Mission, *Space Sci. Rev.*, *195*(1–4), 3–48, doi:10.1007/s11214-015-0139-x.

Krasnopolsky, V. A. (2015), Variations of the HDO/H_2O Ratio in the Martian Atmosphere and Loss of Water from Mars, *Icarus*, *257*, 377–386, doi:10.1016/j.icarus.2015.05.021.

Krasnopolsky, V. A., M. J. Mumma, and G. R. Gladstone (1998), Detection of Atomic Deuterium in the Upper Atmosphere of Mars, *Science*, *280*, 1576–1580, doi:10.1126/science.280.5369.1576.

Lillis, R., et al. (2015), Characterizing Atmospheric Escape from Mars Today and Through Time, with MAVEN, *Sp. Sci. Rev.*, *195*(357–422), 2015, doi:10.1007/s11214-015-0165-8.

Maltagliati, L., F. Montmessin, O. Korablev, A. Fedorova, F. Forget, A. Maattanen, F. Lefevre, and J.-L. Bertaux (2013), Annual Survey of Water Vapor Vertical Distribution and Water Aerosol Coupling in the Martian Atmosphere Observed by SPICAM/MEX Solar Occultations, *Icarus*, *223*, 942–862, doi:10.1016/j.icarus.2012.12.012.

Mayyasi, M., et al. (2016), IUVS Echelle-Mode Observations of Interplanetary Hydrogen: Standard for Calibration and Reference for Cavity Variations between Earth and Mars during MAVEN Cruise, *J. Geophys. Res. Space Physics*, *122*, doi:10.1002/2016JA023466.

McClintock, W. E., N. M. Schneider, G. M. Holsclaw, J. T. Clarke, A. C. Hoskins, I. Stewart, F. Montmessin, R. V. Yelle, and J. Deighan (2015), The Imaging Ultraviolet Spectrograph (IUVS) for the MAVEN Mission, *Space Sci. Rev.*, *195*, 75–124, doi:10.1007/s11214-014-0098-7.

Montmessin, F., T. Fouchet, and F. Forget (2005), Modeling the Annual Cycle of HDO in the Martian Atmosphere, *J. Geophys. Res.*, *110*, E03006, doi:10.1029/2004JE002357.

Owen, T., J. P. Maillard, C. de Bergh, and B. Lutz (1988), Deuterium on Mars: The Abundance of HDO and the Value of D/H, *Science*, *240*, 1767–1770, doi:10.1126/science.240.4860.1767.

Quemerais, E., and J. L. Bertaux (1993), Radiative Transfer in the Interplanetary Medium at Lyman Alpha, *Astron. Astrophys.*, *277*, 283–301.

Rottman, G. J., N. W. Thomas, and W. McClintock (2006), SORCE solar UV irradiance results, *Adv. Space Sci.*, *37*, 201–208, doi:10.1016/j.asr.2005.02.072.

Villanueva, G., M. Mumma, R. Novak, H. U. Kaufl, P. Hartogh, T. Encrenaz, A. Tokunaga, A. Khayat, and M. D. Smith (2015), Strong Water Isotopic Anomalies in the Martian Atmosphere: Probing Current and Ancient Reservoirs, *Science*, *348*(6231), 218–221, doi:10.1126/science.aaa3630.

Yung, Y. L., and D. M. Kass (1998), Deuteronomy?: A Puzzle of Deuterium and Oxygen on Mars, *Science*, *280*, 1545–1546, doi:10.1126/science.280.5369.1545.

Yung, Y. L., J. S. Wed, J. Pinto, M. Allen, K. Pierce, and S. Paulson (1988), HDO in the Martian Atmosphere: Implications for the Abundance of Crustal Water, *Icarus*, *76*, 146–159, doi:10.1016/0019-1035(88)90147-9.